SCIENTIFIC REPORTS

A high-throughput three-dimensional cell migration assay for toxicity screening with mobile device-based macroscopic image analysis

David M. Timm, M. S.[1,2]*, Jianbo Chen, B. S.[1,2]*, David Sing, B. S.[2,3], Jacob A. Gage, B. S.[2], William L. Haisler, B. S.[2,3], Shane K. Neeley, B. A.[2,3], Robert M. Raphael, Ph. D.[3], Mehdi Dehghani, Ph. D.[4], Kevin P. Rosenblatt, M. D. Ph. D.[4], T. C. Killian, Ph. D.[1], Hubert Tseng, Ph. D.[2] & Glauco R. Souza, Ph. D.[2]

[1]Department of Physics, Rice University, Houston, TX 77005 USA, [2]Nano3D Biosciences (n3D), Houston, TX 77030 USA, [3]Department of Bioengineering, Rice University, Houston, TX 77005 USA, [4]Brown Foundation Institute of Molecular Medicine for the Prevention of Human Diseases, University of Texas Health Science Center, Houston, TX 77030 USA.

There is a growing demand for *in vitro* assays for toxicity screening in three-dimensional (3D) environments. In this study, 3D cell culture using magnetic levitation was used to create an assay in which cells are patterned into 3D rings that close over time. The rate of closure was determined from time-lapse images taken with a mobile device and related to drug concentration. Rings of human embryonic kidney cells (HEK293) and tracheal smooth muscle cells (SMCs) were tested with ibuprofen and sodium dodecyl sulfate (SDS). Ring closure correlated with the viability and migration of cells in 2D. Images taken using a mobile device were similar in analysis to images taken with a microscope. Ring closure may serve as a promising label-free and quantitative assay for high-throughput *in vivo* toxicity in 3D cultures.

Screening for toxicity plays an important role in the drug development pipeline, as it accounts for 20% of total failures of candidate compounds[1]. Improvements in this process could significantly reduce the cost and time-to-market of new therapies. Common screens for drug toxicity use animal models that are similar in composition and structure to the human tissue they represent. However, these models are expensive, time-consuming, low-throughput, ethically challenging, vary widely in results between species, and predict human toxicity with varied success[2–5]. *In vitro* assays have been used as early screens and cheaper alternatives to animal models, but they predominantly use two dimensional (2D) environments that do not accurately replicate the human tissue they purport to represent. In particular, 2D models have different spatial gradients of soluble factor concentrations[6] and substrate stiffnesses[7–9] than those of native tissue, and they do not support the wide array of cell-cell and cell-matrix interactions that cells natively experience[10–12]. As a result, biomedical research has moved towards the use of three-dimensional (3D) models, which can more accurately match the structure and bio-chemical environment of native tissue to better predict *in vivo* toxicity[6,7,10,11,13,14].

One such method to construct 3D models is magnetic levitation[15–18]. In magnetic levitation, cells are incubated with a magnetic nanoparticle assembly consisting of gold nanoparticles, poly-L-lysine, and magnetic iron oxide that non-specifically and electrostatically binds to cells[15,19–21]. These nanoparticles are nontoxic and do not induce an inflammatory cytokine (IL-6, IL-8) response by cells[22,23]. By binding to the nanoparticles, the cells become magnetic and can be manipulated with the external application of a magnetic field. In particular, cells are levitated from the bottom surface, where they interact and aggregate with each other to form larger 3D cultures. This method has been shown to induce the formation of extracellular matrix (ECM) within hours after levitation by the magnetic field and maintain cellular phenotype for days[22]. The magnetic nanoparticles act at the cellular level, allowing for these cultures to be scaled down in size for high-throughput screening. In addition, spatial control allows researchers to tailor assays to particular needs[15,22,24]. Overall, magnetic levitation would seem ideal to replicate cellular environments with relevant ECM and cell-cell interactions that could accurately predict *in vivo* toxicity and efficiently screen candidate compounds.
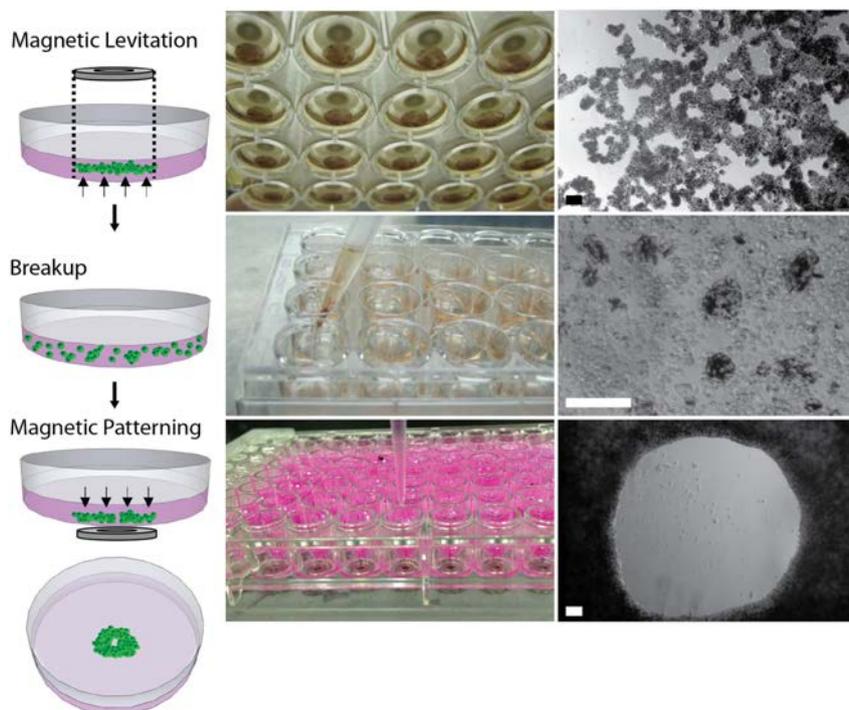
Figure 1 | Schematic for preparing the ring closure assay (left) with corresponding images (center) and brightfield images of 3D cultures of HEK293s (right) for each step. First, cells are levitated to induce ECM formation. Then, cells are mechanically disrupted using pipette action, and patterned into ring shapes. After removing the magnetic field, the rings will close over time, and the rate of closure is measured as a function of drug concentration. Scale bar = 100 μm.

This study describes the use of magnetic levitation in a novel 3D assay for drug toxicity screening (Fig. 1). In the assay, cells are magnetically levitated to form 3D structures with ECM, and then magnetically patterned into 3D ring-shaped cultures. When the magnetic field is removed, the rings close over time due to cell migration and proliferation, and cell-cell and cell-ECM interactions. Ring closure is similar to wound healing, which is commonly tested in 2D to study cell migration[25–28]. The rate of ring closure, found by measuring the outer diameter of the ring over time, can vary with exposure to drugs at different concentrations. Generally, with increasing and more toxic concentrations of a particular drug, cells will close at a slower rate as they become less viable and migratory[25,26]. From the rate of closure, characteristic values such as half maximal inhibitory concentrations (IC_{50}) can be found.

In addition, this assay utilizes mobile devices for image capture (Fig. 2). The use of mobile devices allows for compact and environmental experiments, while forgoing the need for large and expensive imaging equipment such as microscopes. This system is possible because the dark brown color of the nanoparticles and the density of the 3D culture distinguish the 3D culture and provide contrast against the surrounding media. Commonly available mobile devices have cameras with sufficient resolution to capture individual wells within whole plates, and these mobile devices can be programmed to take images at specific timepoints. This method eliminates the need to image cultures under a microscope at multiple timepoints, which reduces the risk of contamination from moving plates in and out of sterile environments, as well as the labor required for an assay.

In this study, ring closure was demonstrated using human embryonic kidney cells (HEK293) and human primary tracheal smooth muscle cells (SMC) with ibuprofen, a known nephrotoxic drug[29–31], and sodium dodecyl sulfate (SDS), a detergent commonly used to denature proteins for electrophoresis, and commonly used as a positive control for toxicity testing[32]. Measurements from the mobile device-based image capture system were compared to measurements from the images captured on a microscope. Additionally, ring closure was also compared to other common assays and markers used for drug toxicity, including cell migration and viability in both 2D and 3D. This study demonstrates the simplicity of ring closure with mobile device-based image analysis, and its potential utility as a 3D *in vitro* assay for toxicity screening.

Results

Ring closure. Ring closure was performed to test the toxicity of ibuprofen and SDS on HEK293s and SMCs. Both cell types were successfully cultured in 3D using magnetic levitation, in which they formed dense and thick 3D cultures. They were then disrupted into smaller 3D structures that were next patterned into a larger 3D ring-shaped culture (Fig. 1). These rings closed over time, and with increasing amounts of ibuprofen and SDS (n = 3 per concentration), the rate of ring closure decreased (Fig. 3). Rings of
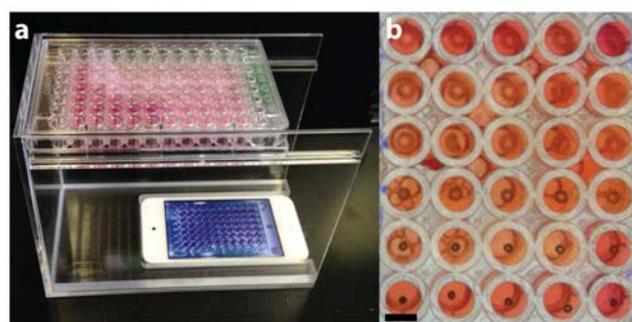

Figure 2 | (a) The mobile device-based imaging setup. The 96-well plate is placed on the top of the setup. At the bottom of the setup sits the mobile device with the camera facing upwards to image the whole plate. (b) A sample image taken with the mobile device of 30 rings of HEK293s and ibuprofen. Note the dark color and the resolution of the rings within the media. Scale bar = 5 mm.

HEK293s closed over the course of 4 days, while rings of SMCs closed within 9 hours.

Comparison of image capture using mobile device and microscope. The analysis of images of rings of HEK293s was compared between those captured using the mobile device-based system and those captured using a traditional microscope after 3 days of exposure to ibuprofen (n = 3 per concentration, Fig. 4). The images taken with the mobile device were able to resolve the dark brown rings within the lightly colored media. In rings of HEK293s, no significant difference was observed up to 1.25 mM ibuprofen in outer diameter between images measured with either the mobile device or the microscope. At higher concentrations, for which the ring did not close, the outer diameter was not measurable with the microscope due to the limited field of view at its lowest magnification (2.5x), so ring diameter was only measured on the microscope up to 1.25 mM.

Rate of ring closure. The rate of ring closure for a particular drug concentration was found from a linear least-squares fit of the outer diameter versus time (Fig. 3, see Supplemental Table S5 for r^2's of

linear least-squares fits). Closure rates were then plotted against drug concentration (Fig. 5). The data were fit to a Boltzmann sigmoidal curve (see Supplemental Table S6 for r^2's of the sigmoidal fits), from which the IC_{50}'s were found (Table 1).

Cell migration and ring closure. Ring closure was compared to a 2D cell migration assay using the same cell types and drugs (n = 3 per concentration, Fig. 6). As expected, cell migration in 2D generally decreased with increasing drug concentration in a manner similar to ring closure, although the dose-response curves were statistically different (see Supplementary Tables 1–4 for p-values). With the exception of HEK293s and SDS, higher IC_{50}'s were found from ring closure than from cell migration (Table 1).

Viability and ring closure. Ring closure was also compared to the viability of the same rings, as well as the viability of 2D cultures using the same cell types and drugs (n = 5 per concentration in 3D, n = 6 in 2D, Fig. 7). Both SDS and ibuprofen reduced cell viability with increasing concentration. In general, viability in 2D and 3D strongly correlated with ring closure in all cases, although the dose-response curves in certain cases were statistically different (see Supplementary
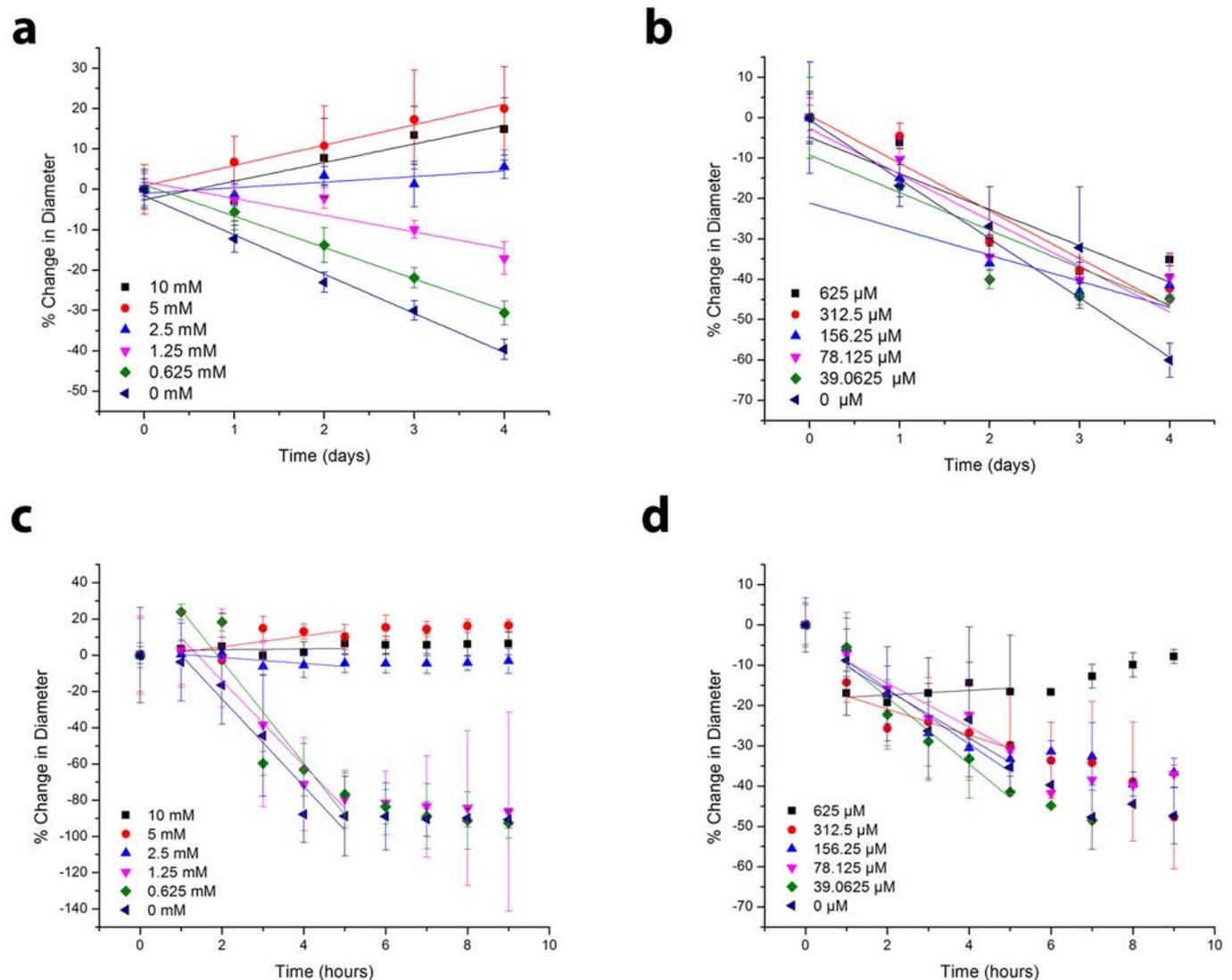

Figure 3 | The outer diameters of rings with HEK293s (a,b) and SMCs (c,d) exposed to either ibuprofen (a,c) and SDS (b,d) as a function of time. The rate of ring closure was found by fitting the outer diameters of each concentration with a linear least-squares fit. Generally, rings of both cell types close over time, and increases in drug concentration lead to slower rates of closure. For SMCs, the rate of closure was found between 1–5 hours, as the rings exposed to ibuprofen stopped closing after 5 hours. Error bars represent standard deviation.
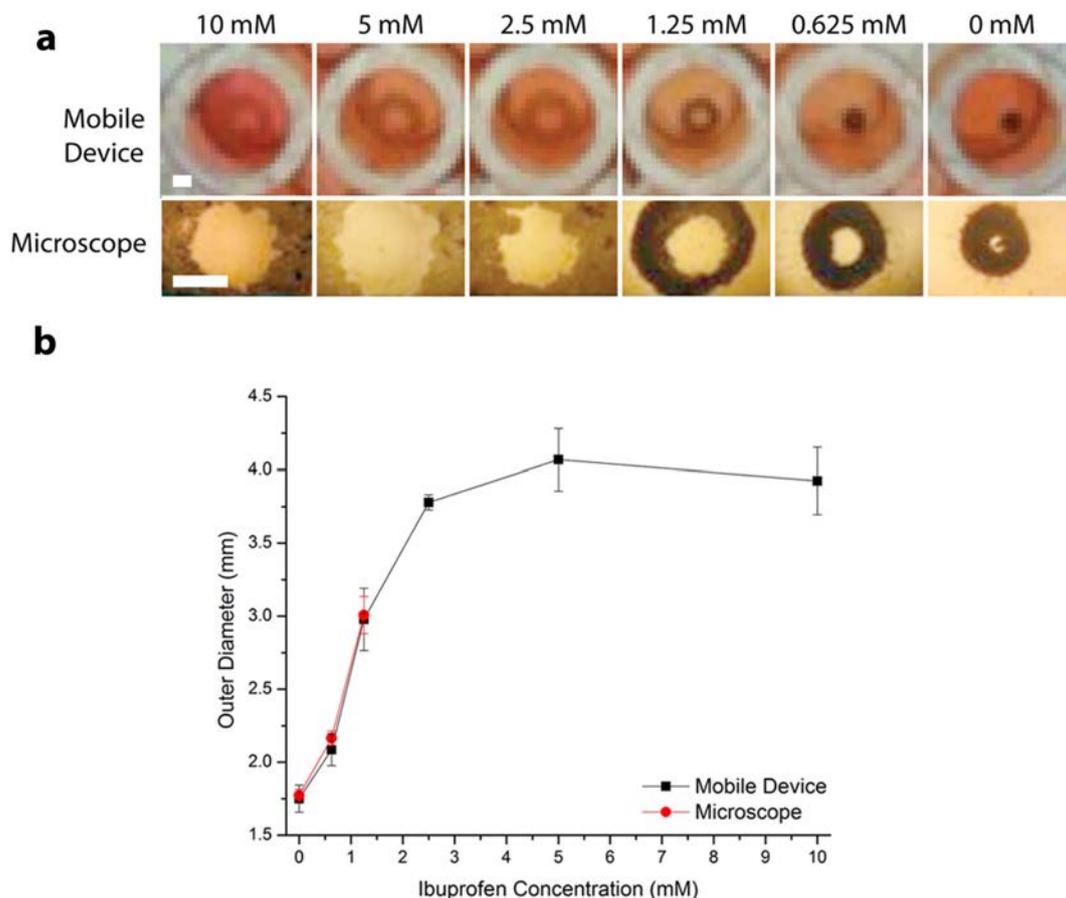
Figure 4 | (a) Images of ring closure using HEK293s and ibuprofen taken with a mobile device (top) and microscope (bottom) after 3 days. Note the resolution and dark color of the rings using the mobile device. (b) Outer ring diameter as a function of ibuprofen concentration using the mobile device (black square) and microscope (red circle) after 3 days of exposure to ibuprofen. There is no significant difference in outer ring diameter between the two methods up to 1.25 mM. At higher concentrations, the outer diameter using the microscope is unable to measured given the limited field of view of the microscope at its lowest magnification (2.5x), and so the ring diameter was only measured up to 1.25 mM using the microscope. Scale bar = 1 mm.

Tables S1–4 for p-values). The IC_{50}'s found from ring closure were higher than those found from 3D and 2D viability for both cell types and drugs except for HEK293s and SDS (Table 1).

Discussion

In this study, an assay for toxicity testing was developed using magnetic levitation. HEK293s and SMCs were magnetically levitated into 3D cultures, then physically disrupted into smaller structures and re-patterned into larger 3D ring-shaped cultures. These rings were next exposed to different concentrations of ibuprofen and SDS, and allowed to close over time. The outer diameter of the ring was imaged using a mobile device-based system, and related to concentration and time. This study demonstrated a novel 3D assay with a mobile device using magnetic levitation with potential use as a screen for drug toxicity.

Magnetic levitation was used to produce a 3D cell culture that could be manipulated with magnetic fields to spatially organize cells into useful, patterned 3D cultures. When patterned into a ring, cells within the 3D culture will close the ring over time as cells migrate and proliferate. This mechanism is similar to that of commonly used wound healing assays, in which cells migrate to close a mechanically or electrically induced hole or linear scratch[25–28]. The basic measurement this assay uses, ring diameter, is macroscopic, label-free, quantifiable, and reproducible. The large size and dark color of the rings facilitated easy measurement. While this study used the rate of ring closure to measure toxicity, other measures could be used, such as the

diameter at a particular timepoint, or a parameter of a non-linear fit to the time-dependent diameter data. This assay also allows for time-based studies within single experiments. Due to the label-free nature of the assay, the closed rings are also available for post-assay experimentation using such techniques as immunohistochemistry[22,33] and Western blotting[24] to delve deeper and explore mechanisms of toxicity. In addition, no expensive analytical equipment, such as a spectrometer, was required to perform this assay.

The assay in this study also utilized a mobile device-based imaging system, which yielded similar results to images taken with a microscope. This method of image acquisition is possible due to the large size of the ring patterns (0.1875" OD, 0.0625" ID) and the computing and camera capabilities of commonly available mobile devices; the mobile device in the system could resolve lines at least 250 ìm wide. Given this capability, while the outer diameter of the ring was measured in this study, other measurements could be taken of the ring, including the inner diameter or area, to measure drug toxicity. The small size of the mobile device setup allowed for the experiment to be performed completely within a standard incubator, allowing for better control of environmental conditions. In addition, the mobile device was programmed to automatically take images at particular timepoints using a freely available application, of which there are several similar applications. Altogether, this system eliminates the need to image the plate under a microscope at multiple timepoints. Along with the possibility that a network connected mobile device could be programmed to send data wirelessly out of the incubator to
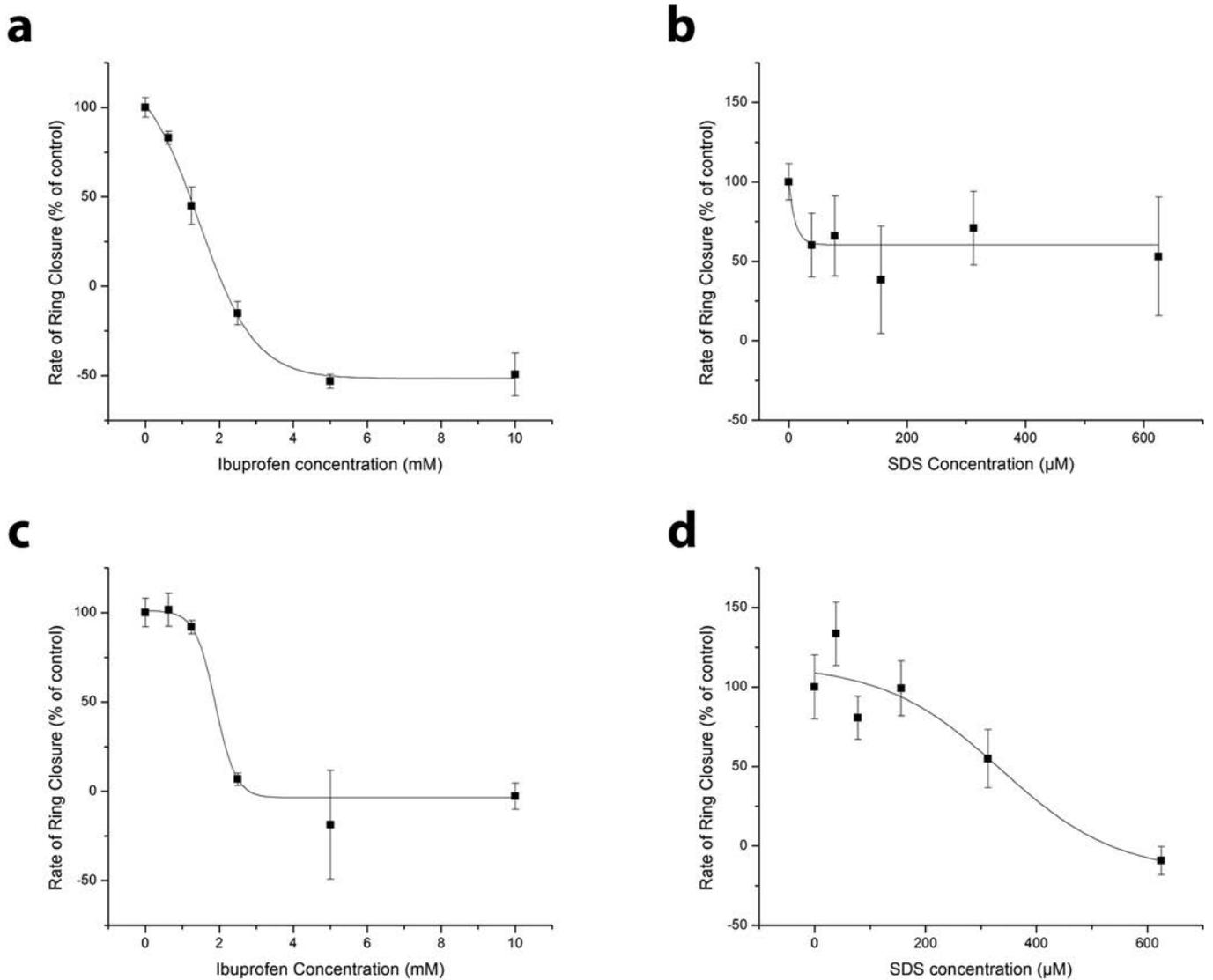
Figure 5 | Dose-response curves of ring closure rates of HEK293s (a,b) and SMCs (c,d) exposed to ibuprofen (a,c) and SDS (b,d). All rates were normalized to control. Error bars represent standard deviation.

another computer for analysis, this system could reduce the risk of contamination associated with taking plates in and out of the incubator. This system could potentially serve as a low-cost and time-saving alternative to large and expensive real-time imaging systems. Smaller rings could be designed and imaged under a microscope or real-time imaging system, but the aforementioned advantages of using the mobile device would be lost. Overall, this mobile device-based imaging system can be used to improve the throughput and efficiency of this assay.

The results of this study showed varied responses of ring closure with HEK293s and SMCs to ibuprofen and SDS compared to cell migration in 2D and cell viability in 2D and 3D. Rings of HEK293s

and SMCs closed at different rates, within 4 days and 9 hours, respectively. For SMCs, the r^2's of the linear least-squares fits were low at higher concentrations of ibuprofen and SDS, but as those rings did not close, it could be assumed that the r^2 reflects the poor integrity and low viability of the rings. In these cases, the ring are loose and create debris due to weakened cell-cell and cell-ECM interactions resulting from toxicity. The free movement of these loose particles likely introduced variability into the time-dependent change in diameter results. Rings of HEK293s did not see such variability, which could possibly be attributed to the differences in ECM composition and cell-ECM interactions between the two cell types and the cultures they created. There was also a difference in closure rates found

Table 1 | IC$_{50}$'s of ibuprofen and SDS with HEK293s and SMCs found using ring closure, cell migration, and 2D and 3D cell viability

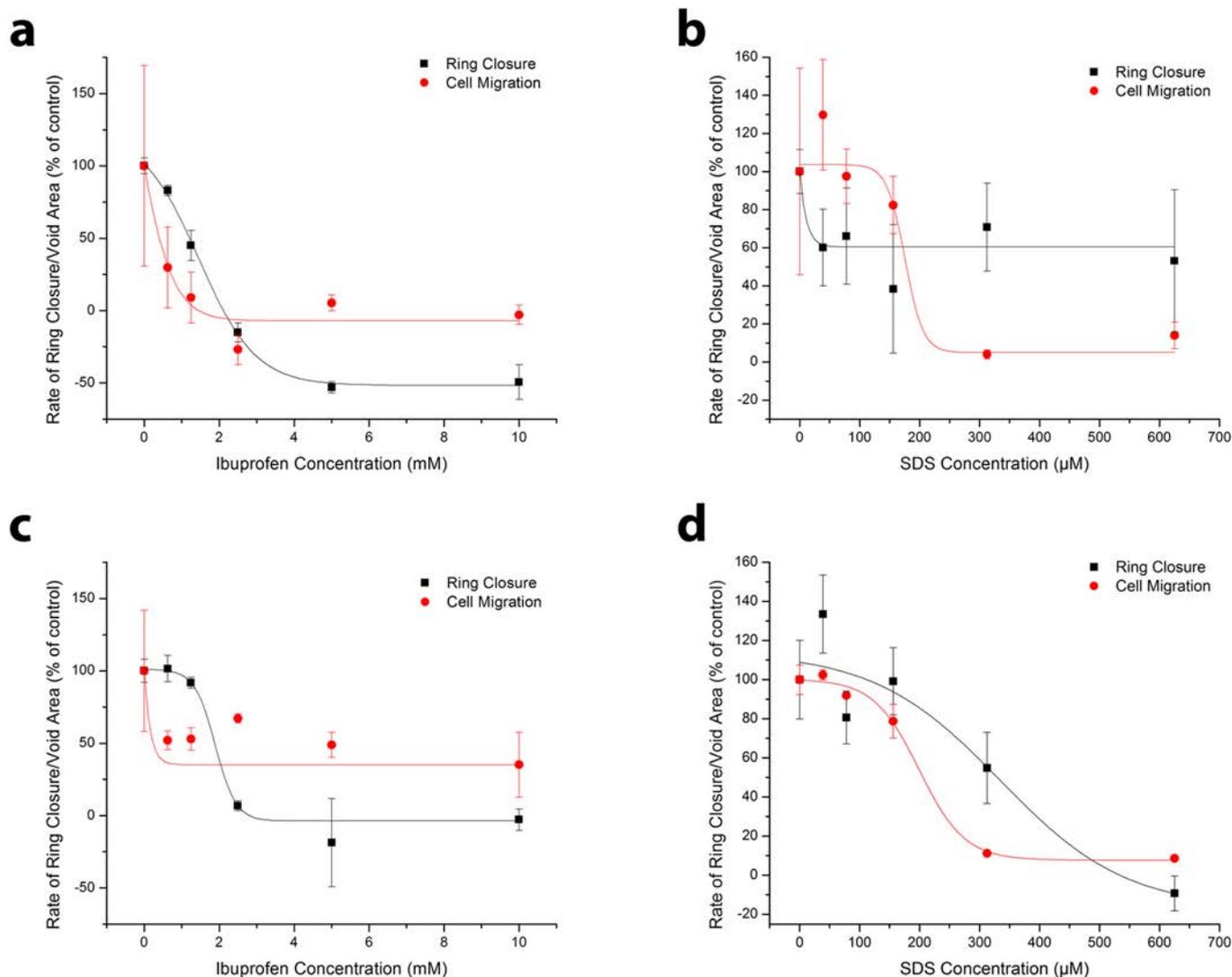| Cell Type	Drug	IC$_{50}$ (mM)			
		Ring Closure	Cell Migration Assay	3D Viability	2D Viability
HEK293	Ibuprofen	1.21	0.41	1.00	0.69
	SDS	0.08	0.18	0.41	0.31
SMC	Ibuprofen	1.88	0.24	0.58	0.48
	SDS	0.33	0.21	0.31	0.29

Figure 6 | Dose-response curves from the ring closure assay (black square) and cell migration assay (red circle) for HEK293s (a,b) and SMCs (c,d) exposed to ibuprofen (a,c) and SDS (b,d). All rates were normalized to control. Error bars represent standard deviation.

between the controls for both drugs, likely due to the difference in control solution, which was either 1% dimethyl sulfoxide (DMSO) for ibuprofen or phosphate buffered saline (PBS) for SDS.

The differences in response found between ring closure and 2D cell migration and viability can partly be explained by the different environments of the two experiments. Cells exhibit widely different behaviors regarding matrix adhesion[10], migration[34], and proliferation[35] between the two environments, likely due to the physical constraints of a structure dense in cells and ECM, and the proximity with more cells in 3D. With regards to drug exposure, cells in a 2D monolayer are exposed to a drug from above, while in 3D, cells are differentially exposed to the drug based on distance from the center. Indeed, previous studies with collagen gels encapsulated with cells[36] or spheroids[37,38] demonstrated lesser effects of drugs on cells in 3D compared to 2D. The differences found between ring closure and 3D viability could possibly be attributed to difficulty of using reagent-based assays on 3D cultures[35], which are limited in their ability to reach the center due to the dense nature of the structures. Furthermore, measuring the viability of the rings required breaking up the cultures, which could have resulted in cell loss. Additional experimentation is required to understand the functional and quantitative relationship between ring closure and cell migration and viability. However, this study was a first step towards evaluating the potential of a ring closure assay for drug toxicity screening. Extra

work will help elucidate cell behavior within the magnetically levitated 3D cultures, and the role of the 3D environment in the toxic response of cells.

In conclusion, ring closure is a label-free, high-content and high-throughput assay for cell migration that incorporates the advantages of a 3D environment. Imaging the assay with a mobile device reduces imaging time under a microscope and may improve the throughput and efficiency of drug toxicity screening. This system may also find further application as a model for wound healing. The resulting assay is a novel approach to recreating native environments *in vitro* to screen and predict human *in vivo* drug toxicity.

Methods

Cell culture. HEK293s (ATCC, Manassas, VA) and SMCs (ScienCell, Carlsbad, CA) were both cultured in Dulbecco's Modified Eagle Medium (DMEM, ScienCell) with 10% fetal bovine serum (FBS, Access Biologicals, Vista, CA) and 1% penicillin/streptomycin (Sigma-Aldrich, St. Louis, MO). Cells were maintained in a humidified environment (37°C, 5% CO_2). HEK293s were used between their fifth and twentieth passage, while SMCs were used between their third and ninth passage.

Magnetic levitation. Magnetic levitation was used to form 3D cultures as has been reported previously in literature[15]. Flasks of HEK293s and SMCs grown in 2D at 70–80% confluence were incubated with a magnetic nanoparticle assembly (8 μL/cm² cell culture area, NanoShuttle, Nano3D Biosciences, Houston, TX) overnight. The next day, the cells were detached from their flasks with trypsin and resuspended in media. The cell suspension was added (2 mL, 600,000 cells/mL) to a well in an ultra-low
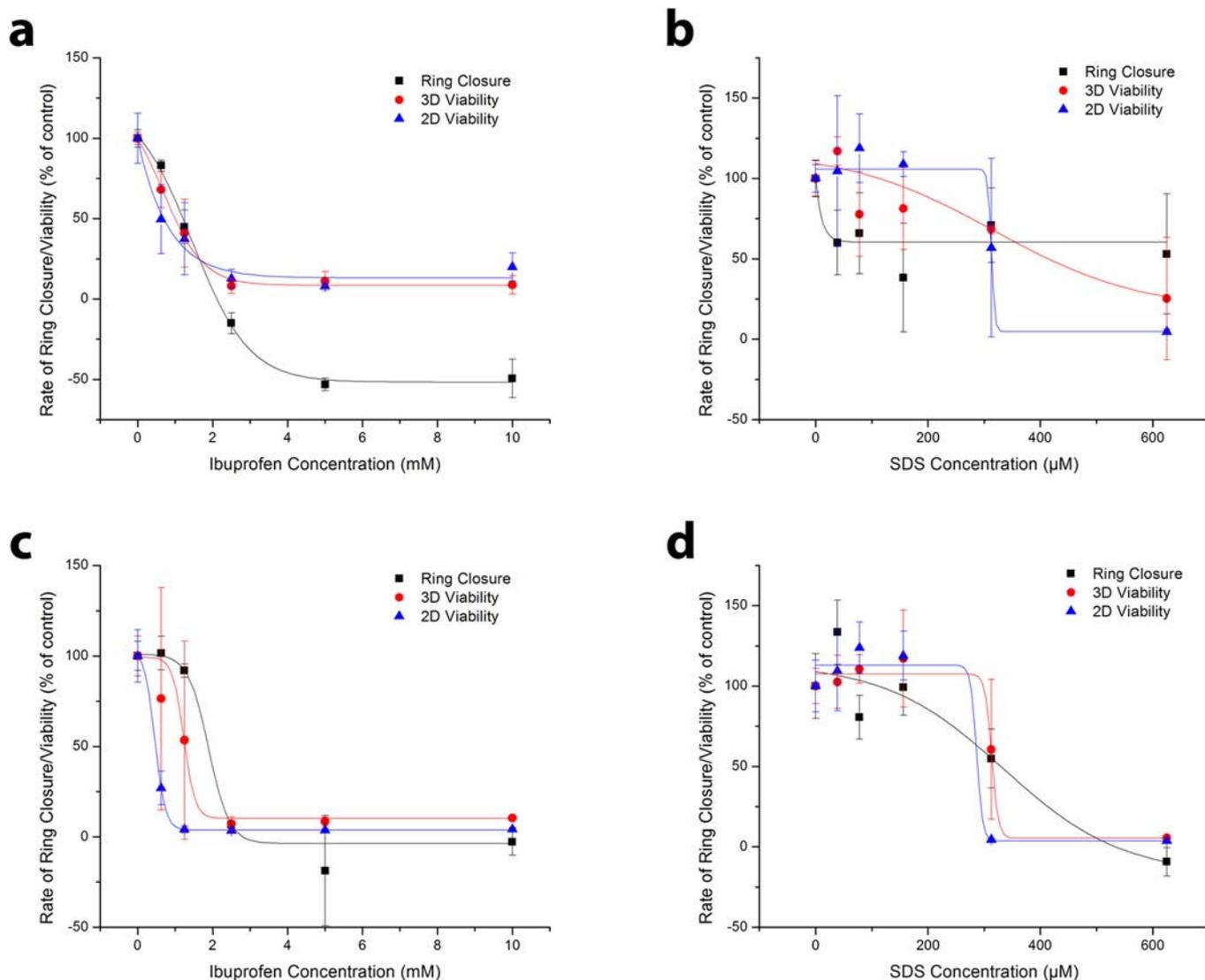
Figure 7 | Dose-response curves from the ring closure assay (black diamond) and viability of 3D cultures (red circle) and 2D cultures (blue triangle) for HEK293s (a,b) and SMCs (c,d) exposed to ibuprofen (a,c) and SDS (b,d). All rates were normalized to control. Error bars represent standard deviation.

attachment 6-well plate (Corning, Tewksbury, MA), and the well plate was closed. A magnetic drive consisting of 6 neodymium magnets was then placed atop the well plate to levitate the cells to the air-liquid interface. These cells are then left to culture overnight in an incubator.

Ring closure. After magnetic levitation, 3D cultures of HEK293s and SMCs were patterned into rings (BiO Assay Ring, Nano3D Biosciences) and allowed to close over time. In this procedure, the 3D cultures of both cell types cultured overnight were broken up physically using pipette action, then transferred to ultra-low attachment 96-well plates (Corning). The cells were distributed to each well (200,000 cells/well) as a volume percentage of the broken up and resuspended 3D culture. The plate was then placed on a magnetic drive of 96 neodymium ring-shaped magnets (0.1875" OD, 0.0625" ID) that attracted the resuspended cultures to the bottom of the plate to form a ring pattern. The plate was left on the magnet for 1 hour to allow for the cells to pattern and reassemble into a competent 3D structure. Next, ibuprofen (0–10 mM in 1% DMSO, Sigma-Aldrich) or SDS (0–625 µM in PBS, Fisher Scientific, Waltham, MA) were added to each well. Negative controls for ibuprofen and SDS were exposed to 1% DMSO and PBS, respectively. The plate was removed from the magnetic drive and the ring-patterned cultures were allowed to close. The outer diameters of these rings were imaged and the outer diameters were measured over time. The percent change in ring diameter was found by normalizing the outer diameters to its initial diameter. To yield a dose response curve, the time rate of ring closure for each drug concentration was found by fitting the outer diameters to a linear least-squares fit (OriginPro, OriginLab, Northampton, MA), then normalized to control. For SMCs, the rates of ring closure was only measured between 1 and 5 hours, when the rate was highest, as SMCs exposed to ibuprofen stopped closing after 5 hours, while for HEK293s, the rates were measured up to 5 days.

Mobile device-based image analysis. Once the rings were formed and exposed to the drug of interest, the rings were imaged using a mobile device (iPod touch, 32 GB, Apple Computer, Cupertino, CA). 96-well plates with the rings inside were placed in a custom polycarbonate apparatus atop the mobile device. A light source (LightPad A920, Artograph Inc., Delano, MN) was then placed atop the plate to illuminate the images. The mobile device was then programmed to take images at particular timepoints using an application (Experimental Assistant, Nano3D Biosciences). In this setting, the mobile device can resolve 250 ìm wide lines on a MIL-STD-150A resolution test pattern (Thorlabs, Newton, NJ). For rings of HEK293s, images were taken every day for 4 days, while for rings of SMCs, images were taken every hour for 9 hours. Afterwards, the images were transferred to a separate computer, where a custom image analysis code written in MATLAB (Mathworks, Natick, MA) was used to measure the diameters of the rings. Briefly, a cropped image of each well was converted to a binary image using a threshold that yielded the ring alone in the well. A circle was drawn around the ring, and the diameter of this circle was recorded as the outer diameter of the ring. Similarly, to compare the performance of the mobile device image capture to a traditional microscope, rings formed with HEK293s and exposed to ibuprofen were imaged under a microscope at the same timepoints, and the outer diameters were measured using ImageJ (NIH, Bethesda, MD).

Cell migration assay. Ring closure was compared to a cell migration assay in 2D (Oris Cell Migration Assay, Platypus Technologies, Madison, WI). Briefly, HEK293s and SMCs were seeded in 96-well plates at a concentration of 50,000 cells/well in 100 µL of media (n = 3 per cell type, drug). The cells were seeded around a cylindrical stopper to create a void at the center of the well. The cells were left to adhere overnight, after which either ibuprofen or SDS was added, and the stopper was removed, allowing the cells to migrate and close the void. The inner diameter of the void was imaged under a

microscope after 72 hours and the inner diameter was measured using ImageJ. The change in diameter was then calculated for each drug concentration and cell type, then normalized to control.

Viability assay. The viability of cells within the ring, as well as cells in 2D, was measured using the CellTiter-Blue assay (Promega, Madison, WI). HEK293s were magnetically levitated as previously described for 24 hours, then physically disrupted and distributed into a 96-well plate (150,000 cells/well). Next, the cells were patterned on ring-shaped magnets for 1 hour. Either ibuprofen or SDS was then added, and the plate was removed off the magnetic drive to close. The rings were allowed to close for 4 days. In addition, the viability of HEK293s in 2D with varying ibuprofen concentration was measured. HEK293s were seeded into a 96-well plate (2,500 cells/well). Ibuprofen was immediately added, and the cells were allowed to grow for 72 hours, with a media change at 48 hours. To each well to be assayed in 2D or 3D, the media was replaced with 100 μL fresh media, and 20 μL of reagent was added. The plates were incubated with the reagent at 37°C for 4 hours. For 3D cultures, the cultures were physically broken up using pipette action. The viability in the well plates were then read on a fluorescent plate reader (excitation/emission 560/590 nm), then normalized to control.

Data analysis. Dose response curves from each assay were fit to a Boltzmann sigmoidal function (OriginPro), from which the IC_{50} was calculated. A one-way analysis of variance (ANOVA) was used to compare the analysis of images from the mobile device to images from the microscope. Two-way ANOVA tests were performed on the dose-response curves for the effects of assay and concentration. A Tukey's test was performed post-hoc to compare assays. Significance was defined as $p < 0.05$. All statistical analysis was performed using OriginPro. Error bars in figures represent standard deviation. See Supplementary Table 1 for p-values between assays.

1. Kola, I. & Landis, J. Can the pharmaceutical industry reduce attrition rates? *Nat Rev Drug Discov* **3**, 711–5 (2004).
2. Sun, H., Xia, M., Austin, C. P. & Huang, R. Paradigm shift in toxicity testing and modeling. *AAPS J* **14**, 473–80 (2012).
3. Bhogal, N. Immunotoxicity and immunogenicity of biopharmaceuticals: design concepts and safety assessment. *Curr Drug Saf* **5**, 293–307 (2010).
4. Perez, R. & Davis, S. C. Relevance of Animal Models for Wound Healing. *Wounds* **20**, 3–8 (2008).
5. Jelovsek, F. R., Mattison, D. R. & Chen, J. J. Prediction of risk for human developmental toxicity: how important are animal studies for hazard identification? *Obstet Gynecol* **74**, 624–36 (1989).
6. Zhang, S. Beyond the Petri dish. *Nat Biotechnol* **22**, 151–2 (2004).
7. Griffith, L. G. & Swartz, M. A. Capturing complex 3D tissue physiology in vitro. *Nat Rev Mol Cell Biol* **7**, 211–24 (2006).
8. Peyton, S. R., Kim, P. D., Ghajar, C. M., Seliktar, D. & Putnam, A. J. The effects of matrix stiffness and RhoA on the phenotypic plasticity of smooth muscle cells in a 3-D biosynthetic hydrogel system. *Biomaterials* **29**, 2597–607 (2008).
9. Pedersen, J. A. & Swartz, M. A. Mechanobiology in the third dimension. *Ann Biomed Eng* **33**, 1469–90 (2005).
10. Cukierman, E., Pankov, R., Stevens, D. R. & Yamada, K. M. Taking cell-matrix adhesions to the third dimension. *Science* **294**, 1708–12 (2001).
11. Pampaloni, F., Reynaud, E. G. & Stelzer, E. H. K. The third dimension bridges the gap between cell culture and live tissue. *Nat Rev Mol Cell Biol* **8**, 839–45 (2007).
12. Kleinman, H. K., Philp, D. & Hoffman, M. P. Role of the extracellular matrix in morphogenesis. *Curr Opin Biotechnol* **14**, 526–32 (2003).
13. Abbott, A. Cell culture: biology's new dimension. *Nature* **424**, 870–2 (2003).
14. Atala, A. Engineering tissues, organs and cells. *J Tissue Eng Regen Med* **1**, 83–96 (2007).
15. Souza, G. R. et al. Three-dimensional tissue culture based on magnetic cell levitation. *Nat Nanotechnol* **5**, 291–6 (2010).
16. Marx, V. Cell culture: a better brew. *Nature* **496**, 253–8 (2013).
17. Becker, J. L. & Souza, G. R. Using space-based investigations to inform cancer research on Earth. *Nat Rev Cancer* **13**, 315–27 (2013).
18. Haisler, W. L. et al. Three-dimensional cell culturing by magnetic levitation. *Nat Protoc* **8**, 1940–9 (2013).
19. Souza, G. R. et al. Bottom-up assembly of hydrogels from bacteriophage and Au nanoparticles: the effect of cis- and trans-acting factors. *PLoS One* **3**, e2242 (2008).
20. Souza, G. R. et al. Networks of gold nanoparticles and bacteriophage as biological sensors and cell-targeting agents. *Proc Natl Acad Sci U S A* **103**, 1215–20 (2006).
21. Hajitou, A. et al. A hybrid vector for ligand-directed tumor targeting and molecular imaging. *Cell* **125**, 385–98 (2006).
22. Tseng, H. et al. Assembly of a three-dimensional multitype bronchiole coculture model using magnetic levitation. *Tissue Eng Part C Methods* **19**, 665–75 (2013).
23. Tseng, H. et al. A three-dimensional co-culture model of the aortic valve using magnetic levitation. *Acta Biomater* In press (2013).
24. Molina, J. R., Hayashi, Y., Stephens, C. & Georgescu, M.-M. Invasive glioblastoma cells acquire stemness and increased Akt activation. *Neoplasia* **12**, 453–63 (2010).
25. Yarrow, J. C., Perlman, Z. E., Westwood, N. J. & Mitchison, T. J. A high-throughput cell migration assay using scratch wound healing, a comparison of image-based readout methods. *BMC Biotechnol* **4**, 21 (2004).
26. Soderholm, J. & Heald, R. Scratch n' screen for inhibitors of cell migration. *Chem Biol* **12**, 263–5 (2005).
27. Huang, C., Rajfur, Z., Borchers, C., Schaller, M. D. & Jacobson, K. JNK phosphorylates paxillin and regulates cell migration. *Nature* **424**, 219–223 (2003).
28. Lampugnani, M. G. Cell migration into a wounded area in vitro. *Methods Mol Biol* **96**, 177–82 (1999).
29. Khan, K. N. M., Paulson, S. K., Verburg, K. M., Lefkowith, J. B. & Maziasz, T. J. Pharmacology of cyclooxygenase-2 inhibition in the kidney. *Kidney Int* **61**, 1210–9 (2002).
30. Guo, X. & Nzerue, C. How to prevent, recognize, and treat drug-induced nephrotoxicity. *Cleve Clin J Med* **69**, 289–90, 293–4, 296–7 passim (2002).
31. Harirforoosh, S. & Jamali, F. Renal adverse effects of nonsteroidal anti-inflammatory drugs. *Expert Opin Drug Saf* **8**, 669–81 (2009).
32. Alberts, B. et al. *Molecular Biology of the Cell.* (Garland Science, 2002).
33. Daquinag, A. C., Souza, G. R. & Kolonin, M. G. Adipose tissue engineering in three-dimensional levitation tissue culture system based on magnetic nanoparticles. *Tissue Eng Part C Methods* **19**, 336–44 (2013).
34. Zaman, M. H., Kamm, R. D., Matsudaira, P. & Lauffenburger, D. a. Computational model for cell migration in three-dimensional matrices. *Biophys J* **89**, 1389–97 (2005).
35. Ng, K. W., Leong, D. T. W. & Hutmacher, D. W. The challenge to measure cell proliferation in two and three dimensions. *Tissue Eng* **11**, 182–91 (2005).
36. Monzack, E. L., Gu, X. & Masters, K. S. Efficacy of simvastatin treatment of valvular interstitial cells varies with the extracellular environment. *Arterioscler Thromb Vasc Biol* **29**, 246–53 (2009).
37. Seiler, A. E. M. & Spielmann, H. The validated embryonic stem cell test to predict embryotoxicity in vitro. *Nat Protoc* **6**, 961–78 (2011).
38. Friedrich, J., Seidel, C., Ebner, R. & Kunz-Schughart, L. A. Spheroid-based drug screen: considerations and practical approach. *Nat Protoc* **4**, 309–24 (2009).

Acknowledgements

Author contributions

D.M.T. and J.C. equally contributed in performing the majority of the experiments and analysis in Fig. 3–7, with significant help from D.S., J.A.G. and W.L.H. in the design and execution of experiments and from S.K.N. and H.T. in data analysis. M.D., K.P.R., R.M.R., T.C.K. and G.R.S. all contributed to the assay and experimental design. H.T. prepared the manuscript and figures, with help from T.C.K. and G.R.S.

Additional information

Supplementary information accompanies this paper at http://www.nature.com/scientificreports

How to cite this article: Timm, D.M. et al. A high-throughput three-dimensional cell migration assay for toxicity screening with mobile device-based macroscopic image analysis. *Sci. Rep.* **3**, 3000; DOI:10.1038/srep03000 (2013).